2006

An Experiment on Frosting Phenomena in a Fin Bundle

Shigeru Koyama
Kyushu University

Donghwi Kim
Kyushu University

Ken Kuwahara
Kyushu University

Chieko Kondo
Hitachi Air Conditioning Systems

An Experiment on Frosting Phenomena in a Fin Bundle

*Shigeru KOYAMA[1], Dong-Hwi KIM[1], Ken KUWAHARA[1] and Chieko KONDO[2]

[1] Interdisciplinary Graduate School of Engineering Sciences, Kyushu University
6-1, Kasuga-kohen, Kasuga-shi, Fukuoka 816-8580, Japan
Phone: +81-092-583-7831, Fax: +81-092-583-7833, E-mail: koyama@cm.kyushu-u.ac.jp

[2]Technology Development Dept. Hitachi Air Conditioning Systems Co., Ltd.
390, Shimizumuramatsu, Shizuoka-shi, Shizuoka, 424-0926, Japan
Phone: +81-0543-35-9903, Fax: +81-0543-36-0776,
E-mail: kondou_chieko@cm.shimizu.hitachiacs.co.jp

ABSTRACT

This paper deals with an experimental study on the frosting phenomena using a fin bundle, which is an expanded model for the fins of the heat exchanger. The overall characteristics such as total frost mass, mass flux, pressure drop, sensible and latent heat fluxes and the local characteristics such as local temperature, local heat flux and local frost thickness were investigated under several experimental conditions composed of cooling block temperature, humidity and velocity of air. It was found that the cooling block temperature and air humidity affect considerably the total frost mass. The mass flux in all of conditions decreased gradually with time, while the pressure drop increased with frost deposition. The sensible heat flux was nearly constant due to the same airflow rate, but the latent heat flux decreased gradually with time. The local heat and mass transfer characteristics were also clarified by developing an approximation equation for the fin temperature and considering the energy and mass balances to the control volume.

1. INTRODUCTION

The heat exchanger for the refrigerator and the air-conditioner has been developed for its high performance, and attained to the acceptable grade. However, there is a problem to be solved for the heat exchanger; that is about 'Frosting phenomena'. The frosting phenomena occur when humid air flows in the heat exchanger, the surface of which is below freezing point temperature. As known well, the frost layer deposited on the surface of heat exchanger deteriorates the thermal performance of heat exchanger owing to thermal resistance and blockage of airflow passage between fins. Therefore, the researches related to the determination both of adequate heat transfer capacity for compensating the performance deterioration of heat exchanger and appropriate defrosting period in the economical point of view is seriously demanded to develop the high efficient heat exchanger under dry and frosting conditions.

The previous researches on the frosting phenomena in the heat exchanger are mainly classified into three fields; 1) frost properties such as heat conductivity and density of frost, 2) frost formation and growth, and 3) heat exchanger performance under frosting conditions.

As the studies belonging to the first classification mentioned above, Yonko and Sepsy (1967) measured the heat conductivity of frost and proposed its correlation as a function of frost density. Hayashi *et al*. (1977) also proposed a correlation of frost density based on the experiment for investigating frost formation. Yang and Lee (2005) also proposed a mathematical model to predict frost properties and heat and mass transfer within the frost layer formed on a cold plate.

Relevant to frost formation and growth, Hayashi *et al*. (1977) observed the process of frost formation and growth and assorted these into three processes according to the elapsed time. The processes divided are crystal growth period, frost layer growth period and frost layer full growth period. O'Neal (1982) proposed the correlations for frost

layer thickness in the range of the Reynolds number both from 4400 to 15900 and above 15900. Sherif *et al*. (1993) simulated the frost formation process employing a semi-empirical transient model for a flat plate under forced convection condition.

In the studies on the heat exchanger performance under frosting conditions, Yanagida (1969) investigated the heat transfer and pressure drop characteristics of close-finned coils operating under frosting conditions. Senshu *et al*. (1990) carried out theoretical and experimental studies using the cross finned tube heat exchanger and proposed the method to predict frosting air condition and averaged frosting mass flux.

O'Neal (1982) reviewed the previous researches on frosting phenomena and pointed out that the detailed data to design air-conditioner in heating mode in winter season are insufficient. Namely, in the case of microscopic study, the conditions are limited to the surface with quite simple geometry at constant temperature. Therefore, he emphasized that the research applicable to the evaporator of air-conditioner is of importance. It means that the research on the frosting from moist air flowing in the small rectangular duct is needed, because the test data in the case of airflow cooled locally through the airflow passage between fins of heat exchanger are insufficient.

By above reason, Koyama *et al.* (2004, 2005a, 2005b) conducted the experimental study for the frosting on an Al flat plate locally cooled in the rectangular duct, and there, investigated the overall geometry of frost layer deposited and the characteristics of heat and mass transfer from humid air. In the present study, the frosting test using an expanded model of the slit fin bundle of heat exchanger has been performed, which is more practical research to develop the high efficient heat exchanger under dry and frosting conditions.

2. EXPERIMENTAL APPARATUS AND METHOD

Fig.1 shows the schematic of the experimental apparatus. The experimental apparatus installed in an air-controlling chamber mainly consists of test section A, orifice B, blower C and suction fan D. The flow rate of humid air flowing

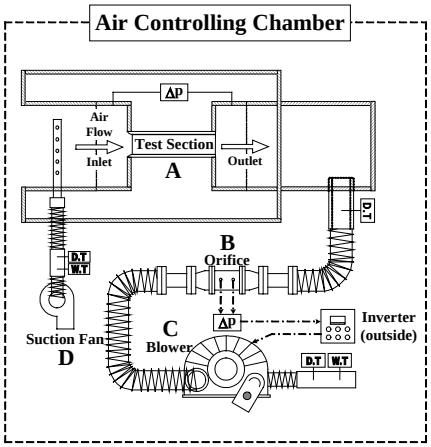

Figure 1: Schematic of the test apparatus

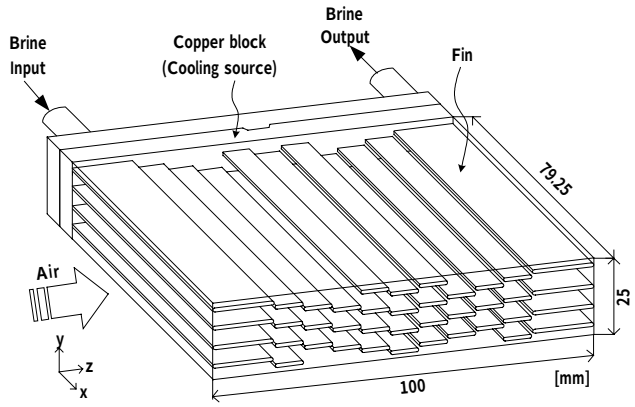

Figure 2: Schematic of the test section

Table 1: Experimental conditions

Test Condition	Air Temperature [^{o}C]		Air Velocity [m/s]	Cooling Block Temperature [^{o}C]
	Dry Bulb	Wet Bulb		
STD	1.99	1.01	1.5	-7.40
HCT	1.98	0.98	1.5	-5.45
LH	1.97	0.49	1.5	-7.81
HH	2.06	1.54	1.5	-7.52
LAV	2.00	1.02	1.0	-8.52
HAV	1.96	1.07	2.0	-7.24

in test section A is measured by orifice B, and blower C is used to flow humid air into test section A. The flow rate of humid air is kept constant by controlling the electric power input of blower C with the inverter. The dry and wet bulb temperature of humid air at the inlet of test section is measured with two sheathed thermocouples (type-K, resolution of ± 0.03 K) by sucking humid air with suction fan D, and controlled by an electric heater, a humidifier and a refrigerator attached to the air-controlling chamber. If the temperature condition of humid air supplied into the test section is stabilized as test conditions, and the experiment is started by flowing brine from the constant temperature bath, which is installed outside the air-controlling chamber, into the test section.

Fig. 2 shows the schematic of the test section. The test section consists of a cooling block, a fin bundle and a rectangular duct made of transparent acrylic resin. The fin bundle is composed of 11 rows by 40 fins inserted into the copper cooling block, and installed inside the rectangular duct. The fin bundle is cooled by flowing brine (ethylene glycol) into the cooling block; where brine is supplied from a constant temperature bath. The width, thickness and length of 8 fins in the 1st and 11th rows are 16.08 mm, 1 mm and 79.25 mm, respectively, and those of the rest 32 fins in the 2nd to 10th rows are 7.5 mm, 1 mm and 79.25 mm, respectively. In order to measure fin temperature distribution, 11 fins in the central part of each row are selected, and five thermocouples with diameter of 0.1 mm (type-T, resolution of ± 0.05 K) in each fin selected are setup. The thermocouples installed to each fin are located at the points of 3, 12, 25, 40 and 70 mm from the base of each fin.

Table 1 lists the experimental conditions. The experimental parameters are cooling block temperature, air humidity and air velocity. In Table 1, STD, HCT, LH, HH, LAV and HAV denote standard, high cooling temperature, low humidity, high humidity, low air velocity and high air velocity conditions, respectively.

Total frost mass, pressure drop between inlet and outlet of the test section, temperature distribution of 11 fins selected and cooling block temperature are measured at each elapsed time of 30, 60, 90 and 120 minutes. Especially in the case of inlet and outlet temperature of the test section, at the inlet of the test section, dry and wet bulb temperature of humid air is measured, and at outlet of the test section, only dry bulb temperature is measured. Also, in order to obtain the humidity ratio at the outlet of the test section, two sheathed thermocouples (type-K, resolution of ± 0.03 K) are installed behind blower C. Total frost mass is determined by measuring total mass of test section before and after each test using a chemical balance (maximum resolution of 0.01 g), and pressure drop between inlet and outlet of the test section is measured using a micro differential manometer (maximum resolution of 0.02 mmAq and maximum range of 50 mmAq).

3. DATA REDUCTION METHOD

Averaged mass flow rate, $\dot{m}_{f,avg}$, is obtained from total frost mass, m_f, and the difference of the operation time, $\Delta\tau$. Also, averaged mass flux, $G_{w,avg}$, is determined from both averaged mass flow rate, $\dot{m}_{f,avg}$, and total heat transfer area, A.

$$\dot{m}_{f,avg} = (m_f\big|_{\tau+\Delta\tau} - m_f\big|_{\tau}) / \Delta\tau \tag{1}$$

$$G_{w,avg} = \dot{m}_{f,avg} / A \tag{2}$$

Total heat flux, q_{tot}, is the sum both of sensible heat flux, q_{sens}, and latent heat flux, q_{lat}.

$$q_{tot} = q_{sens} + q_{lat} = \left\{\rho_a \cdot A_a \cdot u_m \cdot c_p \cdot (T_{db,in} - T_{db,out}) / A\right\} + G_w \cdot h_{sg} \tag{3}$$

Latent heat of sublimation, h_{sg}, is obtained by a correlation used by Ismail-Salinas (1997).

$$h_{sg} = [-0.04667 \times \{1.8 \times (T - 273.15) + 32\} + 1220.1] \times 2322 \tag{4}$$

The approximation equation for fin temperature distribution, which was developed for calculating the local heat flux of fin, is represented as follows:

$$T_w(x) = a \cdot e^{x/L} + b + c \cdot e^{-x/L}. \tag{5}$$

where constants a, b and c are determined by the least square method for fin temperature data measured.

The heat flux in the fin longitudinal direction, $q_{w,x}$, is obtained using Eq. (5) as follows:

$$q_{w,x} = -k_w \cdot \frac{dT_w}{dx} = -\frac{k_w}{L}\left(a \cdot e^{x/L} - c \cdot e^{-x/L}\right). \tag{6}$$

The heat flux from the ambient air to the fin surface, $q_{w,y}$, is also calculated using Eq. (5) as follows:

$$q_{w,y} = \frac{1}{P_f} \cdot \frac{dQ_{w,x}}{dx} = -\frac{k_w A_f}{P_f L^2}\left(a \cdot e^{x/L} + c \cdot e^{-x/L}\right). \tag{7}$$

Fig. 3 shows the control volume in the frosted fin. The energy conservation equation of the airside in the control

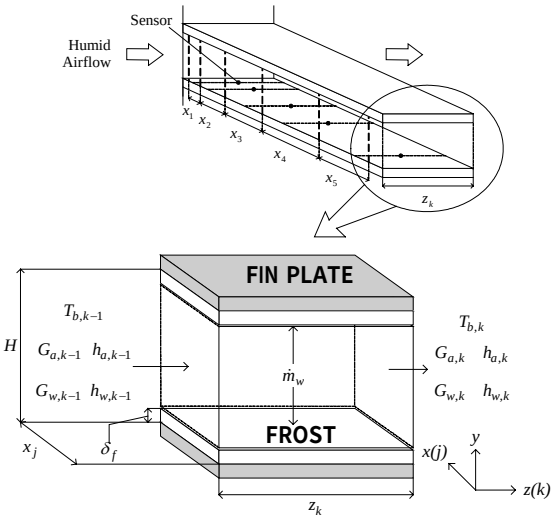

Figure 3: Control volume in the frosted fin

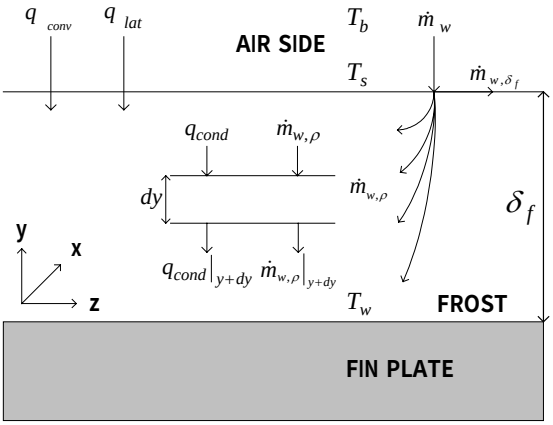

Figure 4: Energy balance both on the frost surface and in the frost layer

volume is described as follows:

$$(G_a c_{pa} + G_w c_{pw})\frac{\Delta T_b}{\Delta z} = -\frac{2}{H}(h_H - \dot{m}_w c_{pw})(T_b - T_s)\,. \tag{8}$$

Fig. 4 represents the energy balance both on the frost surface and in the frost layer. The total heat flux transferred from the moist air to the frost surface includes the sensible heat flux by convection of dry air as well as the latent heat flux by sublimation of water vapor from humid air.

$$q_{tot} = q_{sens} + q_{lat} = h_H (T_b - T_s) + \dot{m}_w h_{sg} \tag{9}$$

$$q_{sens} = q_{conv} = h_H (T_b - T_s) \tag{10}$$

$$q_{lat} = h_M (\chi_b - \chi_s)\cdot h_{sg} = \dot{m}_w \cdot h_{sg} \tag{11}$$

Mass transfer coefficient, h_M, can be determined from heat transfer coefficient, h_H, by the Chilton-Colburn Analogy (or modified Lewis Relation) as

$$h_M = \frac{\rho D}{k} Le^{-1/3} h_H = \frac{\rho c_p D}{k} Le^{-1/3}\frac{h_H}{c_p} = Le^{2/3}\frac{h_H}{c_p}\,. \tag{12}$$

The heat flux transferred from the surface of frost to the fin plate means the heat transfer by conduction through frost layer with certain heat conductivity.

$$q_{tot} = q_{w,y} = k_f\left(\frac{T_s - T_w}{\delta_f}\right) \tag{13}$$

Lee's correlation (1994) is used for the heat conductivity of frost, k_f.

$$k_f = 0.132 + (3.13\times10^{-4}\times\rho_f) + (1.6\times10^{-7}\times\rho_f{}^2) \tag{14}$$

where the density of frost is estimated using the correlation developed by Hayashi *et al.* (1977).

$$\rho_f = 650\exp(0.227 T_s) \tag{15}$$

The mass flow rate per unit area of water vapor from humid air, $\dot{m}_w$, is the sum of mass flux for increasing the frost density, $\dot{m}_{w,\rho}$, and mass flux for increasing the frost thickness, $\dot{m}_{w,\delta f}$.

$$\dot{m}_w = \dot{m}_{w,\rho} + \dot{m}_{w,\delta_f} \tag{16}$$

The mass flux for increasing the frost density, $\dot{m}_{w,\rho}$, used by O'Neal (1982) and the mass flux for increasing the frost thickness, $\dot{m}_{w,\delta f}$, are shown as follows:

$$\dot{m}_{w,\rho} = D_w \left[\frac{1-(\rho_f/\rho_i)}{1+(\rho_f/\rho_i)^{0.5}} \right] \left(\frac{1}{RT_s} \right) \times \left[\frac{h_{sg}}{T_s(\upsilon_w - \upsilon_i)} - \frac{P_w}{T_s} \right] \left(\frac{q_{w,y}}{k_f} \right) \tag{17}$$

$$\dot{m}_{w,\delta_f} = \dot{m}_w - \dot{m}_{w,\rho} . \tag{18}$$

The density of frost is determined from mass flux for increasing the frost density, the elapsed time and the frost thickness. The frost thickness is also obtained from the mass flux for increasing the thickness of frost, the elapsed time and the density of frost.

$$\rho_f\big|_{t+\Delta t} = \rho_f\big|_t + \frac{\dot{m}_{w,\rho} \cdot \Delta\tau}{\delta_f} \tag{19}$$

$$\delta_f\big|_{t+\Delta t} = \delta_f\big|_t + \frac{\dot{m}_{w,\delta_f} \cdot \Delta\tau}{\rho_f} \tag{20}$$

4. EXPERIMENTAL RESULTS

Fig. 5 shows the effect of cooling block temperature on total frost mass, averaged mass flux and pressure drop. It is found that the total frost mass and mass flux are affected considerably by cooling block temperature. It is because water vapor pressure difference between fin surface and ambient humid air is reduced as cooling block temperature becomes higher. It is also found that pressure drop is affected seriously by cooling block temperature due to the blockage of the airflow passage by frost deposited.

Fig. 6 illustrates the effect of air humidity on total frost mass, averaged mass flux and pressure drop. As air humidity becomes higher, total frost mass and averaged mass flux increase due to more abundant supply of water vapor from humid air. It is also found that pressure drop is affected considerably by air humidity owing to the blockage of airflow passage by frost deposited.

Fig. 7 shows the effect of air velocity on frost mass, mass flux and pressure drop. In this experiment, though air velocity affects pressure drop largely, its effect on total frost mass and mass flux is not so large compared with in the cases of conditions for cooling block temperature and air humidity. As air velocity increases, the mass transfer of water vapor to the frost surface is enhanced. On the other hand, temperature difference between ambient humid air and frost surface decreases due to the increase of heat transfer coefficient. This trade-off relation between heat and mass transfer leads to small effect of air velocity on frost mass and mass flux. It is noted that pressure drop is also affected by the blockage of airflow passage due to deposition of frost.

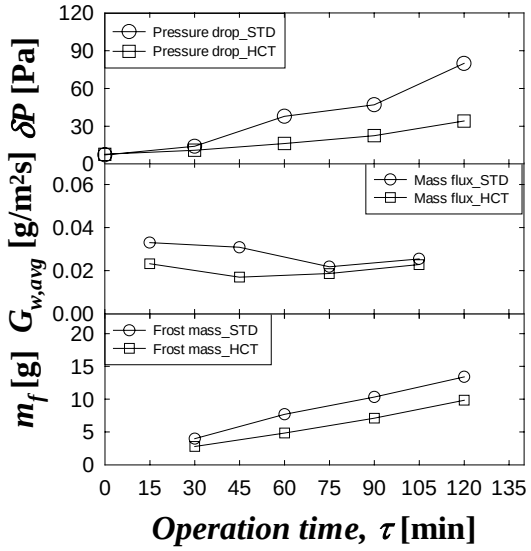

Figure 5: Effect of cooling block temperature on total frost mass, averaged mass flux and pressure drop

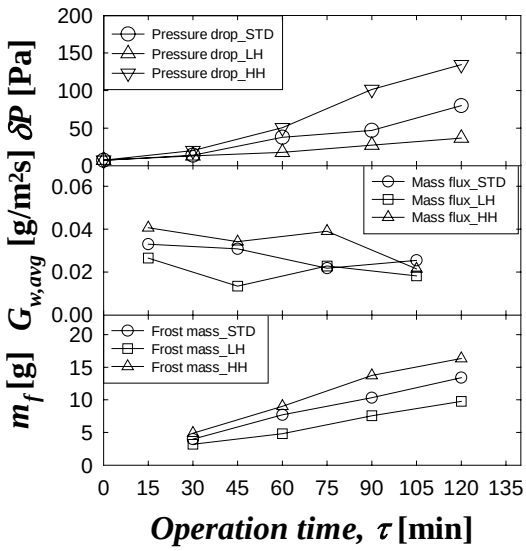

Figure 6: Effect of air humidity on total frost mass, averaged mass flux and pressure drop

Fig. 8 represents the variation of total, sensible and latent heat fluxes with the operation time under standard condition. Sensible heat flux is kept almost constant due to the same airflow rate, while latent heat flux decreases gradually owing to the reduction of water vapor pressure difference between ambient humid air and frost surface. As a result, total heat flux decreases with the operation time.

Fig. 9 shows the temperature variation at each position of 11 fins. As shown, the temperature of fins in upper stream side, fins No. 1-6, is relatively higher than that in down stream side, fins No. 7-11. It is because the fins in upper stream side is in contact with humid air at relatively high temperature compared to down stream side, namely, the fins in down stream side contact with humid air cooled by heat exchange with the fins in upper stream side. Also, the temperatures between fins No. 2 and 3, between fins No. 6 and 7 and also between fins No. 10 and 11, where the airflow direction is abruptly changed by the fin arrangement feature, are higher than those of other positions.

Fig. 10 represents the *y*-directional heat flux, which denotes the heat flux from ambient air to fin surface, at each position at elapsed time of 30 minutes in standard condition. The *y*-directional heat flux profile may be controlled by air flow in fin bundle, which is determined by the fin arrangement.

Fig. 11 shows the frost thickness at each position of 11 fins at elapsed time of 30 minutes in standard condition. The small graph inside the big graph denotes the frost thickness configuration in the fin longitudinal direction. The frost thickness in this study is the averaged value in airflow direction to control volume in Fig. 3. It is found that the frost thickness of fins in down stream side is relatively thicker than that of fins in upper stream side. It means that mass

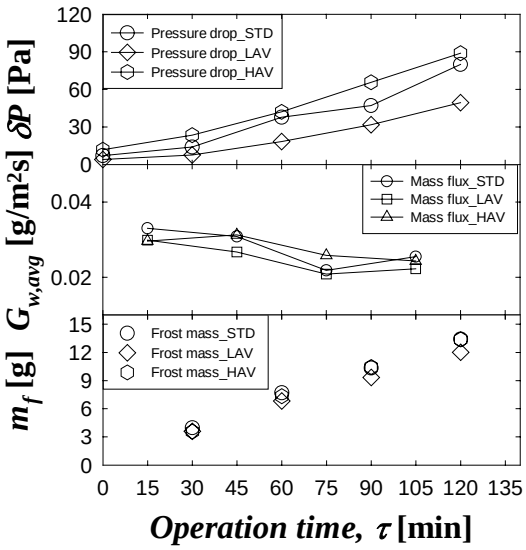

Figure 7: Effect of air velocity on frost mass, mass flux and pressure drop

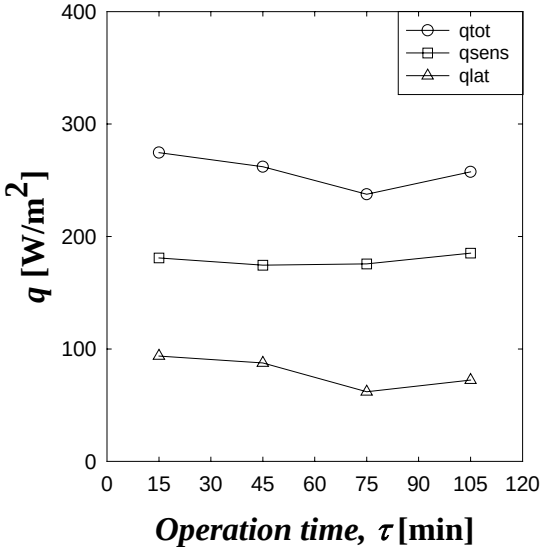

Figure 8: Variation of total, sensible and latent heat fluxes with time under standard condition

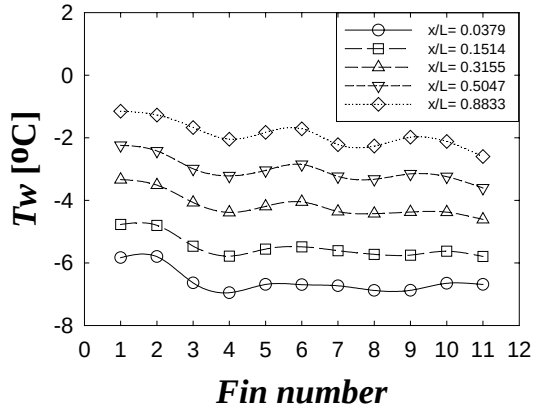

Figure 9: Fin temperature distribution (STD 30min.)

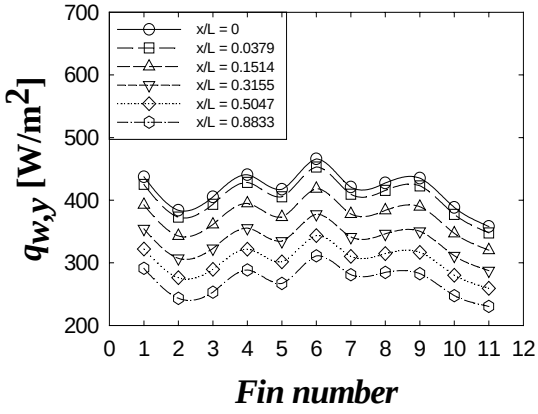

Figure 10: *y*-directional heat flux at elapsed time of 30 minutes in standard condition.

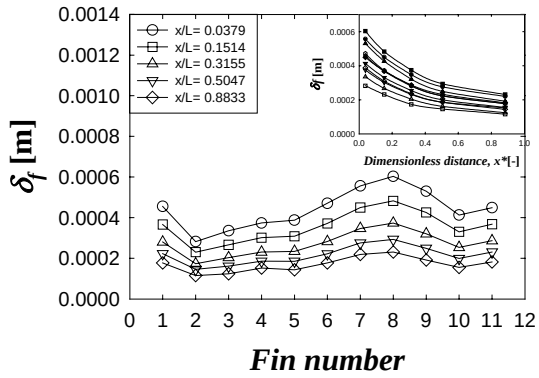

Figure 11: Frost thickness on each fin at elapsed time of 30 minutes in standard condition.

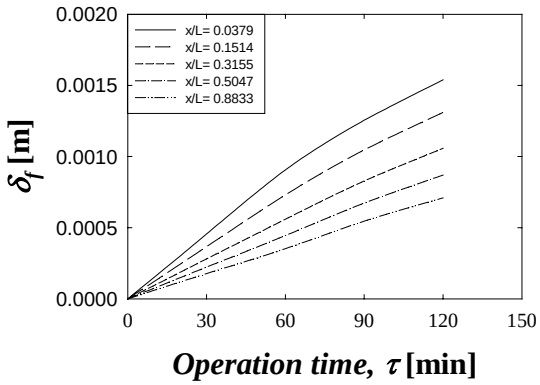

Figure 12: Variation of frost thickness on the fin No.1 with time in standard condition.

transfer occurs more actively in down stream side compared to that in upper stream side. It is also found that the fin No. 1 has thicker frost thickness than other fins in upper stream side due to the leading edge effect.
Fig. 12 shows the variation of frost thickness distribution on the fin No. 1 with the operation time in standard condition. It is found that the frost thickness decreases in x-direction. It is also found that the growth rate of frost gradually decreases with the operation time owing to the decrease of water vapor pressure difference between ambient humid air and frost surface.

5. CONCLUSIONS

The frosting test using an expanded fin bundle in rectangular duct was carried out to obtain the detailed data with respect to the frosting phenomena in the heat exchanger of the heat pump under frosting conditions in the winter season. The results are summarized as follows:

- In the experimental parameters for this test, both cooling block temperature and air humidity considerably affected total frost mass and mass flux.
- Mass transfer had the largest value in the period of 0-30 min., and decreased with time owing to the reduction of the water vapor pressure difference between humid air and frost surface.
- The temperature both of the frost surface and the fin in the upper stream side was higher than that in the down stream side. Also, the fin temperature had the high value in the places where the airflow direction is changed by the fin arrangement.
- The *y*-directional heat flux profile could be controlled by air flow in fin bundle, which was determined by the fin arrangement.
- The frost thickness in down stream side was relatively thicker than that in upper stream side. In upper stream side, the fin No. 1 has the largest frost thickness due to the leading edge effect. Also, the growth rate of frost decreased gradually with the operation time.

NOMENCLATURE

A	total heat transfer area	(m^2)	**Subscripts**	
A_a	cross sectional area of duct	(m^2)	a	air
A_f	cross sectional area of fin	(m^2)	b	bulk air
c_p	isobaric specific heat capacity	(J kg^{-1} K^{-1})	δ_f	frost thickness
D	diffusion coefficient	(m^2 s^{-1})	f	frost
Δ	difference	(-)	i	ice
G_w	mass flux of water vapor	(g m^{-2} s^{-1})	lat	latent
$G_{w,avg}$	averaged mass flux	(g m^{-2} s^{-1})	ρ	frost density

h_{sg}	latent heat of sublimation	(J kg^{-1})	*s*	frost surface
h_H	heat transfer coefficient	(W m^{-2} K^{-2})	*sens*	sensible
h_M	mass transfer coefficient	(kg m^{-2} s^{-1})	*tot*	total
H	height between two fins	(m)	*w*	water vapor, wall
k	heat conductivity	(W m^{-1} K^{-1})	*x*	x-direction
L	fin length	(m)	*y*	y-direction
Le	Lewis number, D/α	(-)	*z*	z-direction
m_f	frost mass	(g)		
$\dot{m}_{f,avg}$	averaged mass flow rate	(g s^{-1})		
$\dot{m}_w$	mass flux of water vapor	(g m^{-2} s^{-1})		
ρ	density	(kg m^{-3})		
R	gas constant for water vapor	(J kg^{-1} K^{-1})		
τ	operation time	(s and min)		
P	pressure			
P_f	perimeter of fin	(m)		
q	heat flux	(W m^{-2})		
Q	heat transfer rate	(W)		
T	temperature	(^{o}C or K)		
u_m	mean air velocity	(m s^{-1})		
υ	specific volume	(m^3 kg^{-1})		
x	distance from the fin base	(m)		

REFERENCES

Yonko, J.D., Sepsy, C.F., 1967, An Investigation of the Thermal conductivity of Frost while Forming on a Flat Horizontal Plate, *ASHRAE Transactions*, vol. 73, no. 2: p. 1.1-1.11.

Hayashi, Y., Aoki, A., Adachi, S., Hori, K., 1977, Study of Frost Properties Correlating with Frost Formation Types, *Journal of Heat Transfer*, no. 99: p. 239-245

Yang, D.K., Lee, K.S., 2005, Modeling of Frosting Behavior on a Cold Plate, *Int. J. Refrig.*, no. 28: p. 396-402

O'Neal, D.L., 1982, The Effect of Frost Formation on the Performance of a Parallel Plate Heat Exchanger, PhD dissertation, Purdue University

Sherif, S.A., Raju, S.P., Padki, M.M., Chan, A.B., 1993, A Semi-Empirical Transient Method for Modeling Frost Formation on a Flat Plate, *Int. J. Refrigeration*, vol. 16, no. 5: p. 321-329

Yanagida, T., 1969, Performance of Frosted Coils, *Refrigeration*, vol. 44, no. 506: p. 1182-1189 (in Japanese)

Senshu, T., Yasuda, H., Oguni, K., Ishibane, K., 1990, Heat Pump Performance under Frosting Conditions: Part1-Heat and Mass Transfer on Cross-Finned Tube Heat Exchangers under Frosting Conditions, *ASHRAE Transaction*, vol. 96, no. 1: p. 324-329

Koyama, S., Kwon, J.T., Kim, D.H., Kondou, C., 2004, An Experimental Study on the Frosting of Laminar Humid Airflow along a Flat Aluminum Plate, *JSRAE Conference*, A317

Kwon, J.T., Koyama, S., Kim, D.H., Kondou, C., 2005, An Experimental Study on Frosting of Laminar Air Flow in a Small Rectangular Duct: part1. Heat and Mass Transfer Characteristics, *The Sixth KSME-JSME Thermal and Fluids Engineering Conference*, EE06

Koyama, S., Kwon, J.T., Kim, D.H., Kondou, C., 2005, An Experimental Study on Frosting of Laminar Air Flow in a Small Rectangular Duct: part2. Frost Thickness Distributions, *The Sixth KSME-JSME Thermal and Fluids Engineering Conference*, EE07

Ismail, K.A.R., Salinas, C., Gonçalves, M.M., 1997, Frost Growth Around a Cylinder in a Wet Air Stream, *Int. J. Refrigeration*, vol. 20, no. 2: p. 106-119

Lee, K.S., Lee, T.H., Kim, W.S., 1994, Heat and Mass Transfer of Parallel Plate Heat Exchanger under Frosting Condition, *SAREK Journal*, vol. 6, no. 2: p. 155-165 (in Korean)